A New Smoothing-Based Farmland Extraction Approach with Vectorization from Raster Remote Sensing Images

Ruoxian Li, Kun Gao(✉), and Zeyang Dou

Key Laboratory of Photoelectronic Imaging Technology and System, Ministry of Education of China, Beijing Institute of Technology, Beijing 100081, China
gaokun@bit.edu.cn

Abstract. With the increasing resolution and application scene of remote sensing images, land and resource investigators begin to consider using these images to investigate crop species, cultivated area and ownership. Instead of manually drawing the boundary of the selected farmland region, an efficient edge-preserving smoothing method for automatically segmenting and extracting the area is proposed, which is performed according to the following three steps: (1) Remove the interference information by image preprocessing. The smoothing algorithm in this process was proposed according to features of the ideal smoothed image and using Maximum a Posteriori estimation model to preserve borderlines of farmland regions; (2) Image segmentation, including threshold and region segmentation using the fixed threshold and the hole removal based on the region growth method respectively after edge and whole image enhancement; (3) Information extraction, including region separation with the Flood Fill method and region vectorization which can reduce the amount of data and make the image to scale arbitrarily by contour tracking after thinning with the Freeman Chain Code. The final results of segmenting and extracting farmland objects with different features from raster remote sensing images demonstrate the correctness and efficiency of the proposed process.

Keywords: Remote sensing image · Edge-preserving smoothing · Farmland region · Image segmentation · Information extraction · Vectorization

1 Introduction

With the development of remote sensing (RS) technology, the accuracy of RS image has been continuously improved, and it has been widely used in military reconnaissance, land resource survey, disaster monitoring, etc. Nowadays, investigators are trying to investigate crop species, cultivated area and ownership through orthoimages of farmland in China. However, due to the complex environment, they need to draw the boundary of the area manually. In view of this inefficient work, automatic farmland extraction approach is in urgent need of research and application.

In order to extract the regional information of farmland, we have to remove the interference caused by the process of image transmission and the land or vegetation texture within the region first. Since the information of edges is important in most

Y. Zhao et al. (Eds.): ICIG 2019, LNCS 11903, pp. 334–346, 2019.
https://doi.org/10.1007/978-3-030-34113-8_28

cases, the traditional smoothing filters such as mean filter, Gaussian filter and median filter are gradually replaced by Laplacian of Gaussian (LoG) operator [1], Bilateral filter [2], total variation [3] and so on. Based on these algorithms, edge-preserving smoothing algorithms with better performance have been proposed. Farbman et al. [4] proposed a flexible filter using the weighted least square (WLS) framework. Zhang et al. [5] proposed the rolling guidance filter (RGF) to separate different scale structures. Dou et al. [6] proposed the truncated total variation to preserve only salient structures. In this paper, we finally designed a new algorithm which is more suitable for farmland based on the advantages of existing algorithms.

Image segmentation and information extraction of farmland should be the important process to realize the automatic farmland extraction. Most of the information extraction algorithms for RS images are oriented to the whole image [7], or segment and extract the region of interest according to the spectral characteristics [8]. The extraction methods for specific objects such as river [9] and road [10] networks are not effective in farmland due to their different object characteristics. Now there are algorithms to achieve fine farmland segmentation by stratified regionalization and local segmentation parameter estimation [11]. In order to draw the boundary of a piece of farmland automatically, we only need to extract the information of the designated one. Therefore, the fine segmentation of all farmland which requires a lot of work is not conducive to practical application. What's more, RS images are stored as raster images generally. Since they have a large amount of data and can not be arbitrarily scaled, we have to vectorize them through thinning-based, contour-based, run-graph-based or other classical vectorization algorithms to save the extraction results.

In this paper, we developed a new smoothing-based automatic farmland segmentation and extraction approach with vectorization from raster RS images. After the regions of interest in images are vectorized and stored, the investigators can directly edit the information of the regions, thus avoiding the influence of the subjective factors and reducing the time needed for information extraction and recording.

2 Methods

The proposed method of farmland segmentation and extraction with vectorization from raster RS images contains three steps: image preprocessing, image segmentation, and information extraction. The specific workflow is shown in Fig. 1. To begin with, the input raster RS image needs to be preprocessed. Then, threshold segmentation and region segmentation can be performed on preprocessed images. Finally, the region of interest is separated from the segmented image by region separation technique. After vectorization, the farmland information of the designated area is extracted, and the vectorized farmland image can be used by land investigators.

2.1 Image Preprocessing

As raster images scanned by aerial or scanner usually contain a lot of redundant information, image noise, etc., which will adversely affect subsequent image processing, it is necessary to preprocess the original image. Since the selected raster image

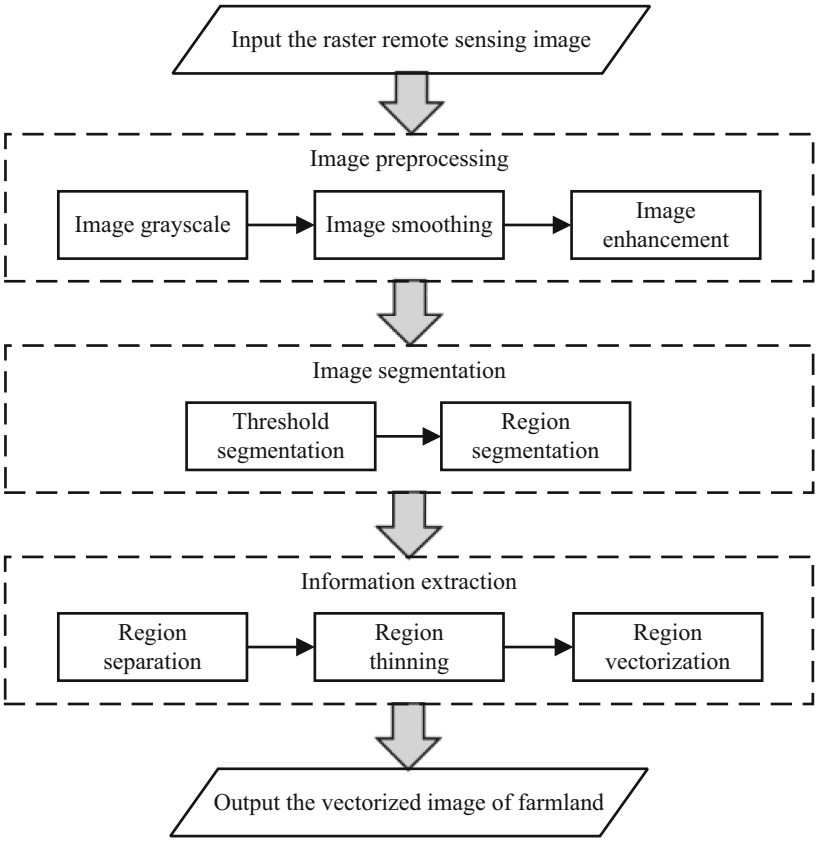

Fig. 1. Workflow of the proposed method.

is orthophoto, image correction is not required. In our proposed method, image preprocessing includes image grayscale, image smoothing and image enhancement to improve the quality of input original image.

Image Grayscale. Grayscale image processing can simplify the image information under the condition of ensuring the integrity of useful information. For the input color image, we use the weighted average method to process the three components of RGB and the result of the sample image can be seen in Fig. 2(a):

$$f(x, y) = 0.21R(x, y) + 0.72G(x, y) + 0.07B(x, y) \quad (1)$$

Image Smoothing. Smoothing images can minimize the ratio of image noise and texture. Since we want to preserve the information of edges, according to the introduction of smoothing algorithms at the beginning, we have tried a lot. Figure 2(b) and

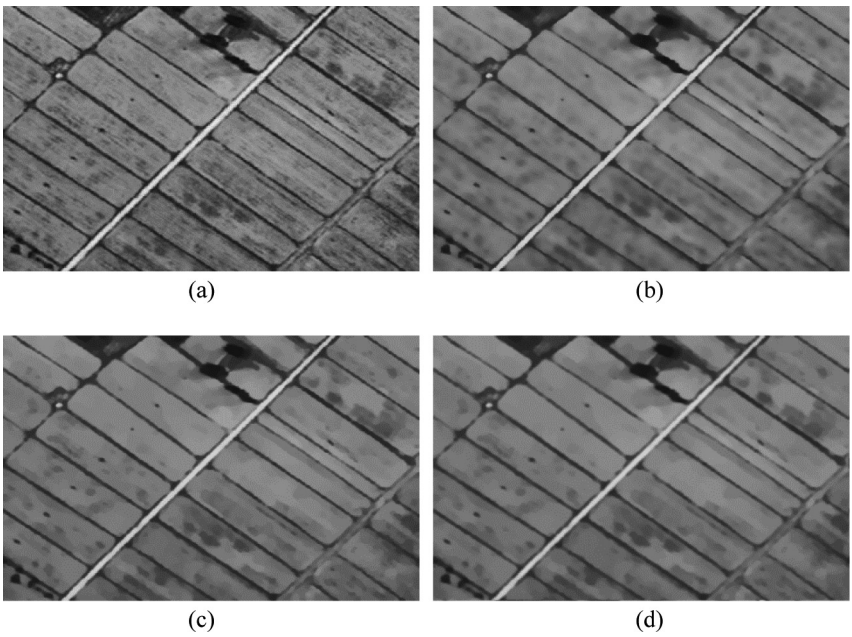

Fig. 2. Image smoothing results comparison. (a) Grayscale input image; (b) Bilateral filter; (c) Total variation; (d) Proposed method.

(c) show the smoothing results of the classical Bilateral filter and total variation algorithms.

Since these classical algorithms can not meet our needs that the texture in the region should be removed better, we consider first defining the characteristics of the ideal smoothed image of the farmland, and then choose the most appropriate method. We used Photoshop to draw the simulated farmland and its ideal smoothed image as shown in Fig. 3(a) and (c), and their histograms of gradient statistics are shown in Fig. 3(b) and (d) respectively.

The gradient of the original image conforms to the Laplace distribution, but that of the smoothed image does not. We denote the input image by f, the smoothed result by u and the pixel value of u is normalized to [0, 1]. The gradient distribution of the smoothed image can be expressed as

$$D(x) = \frac{1}{c} e^{-|T(\nabla u)|} \tag{2}$$

$$s.t.\ \ c = \frac{1}{\int\limits_{\Omega} e^{-|T(\nabla u)|} dxdy} \tag{3}$$

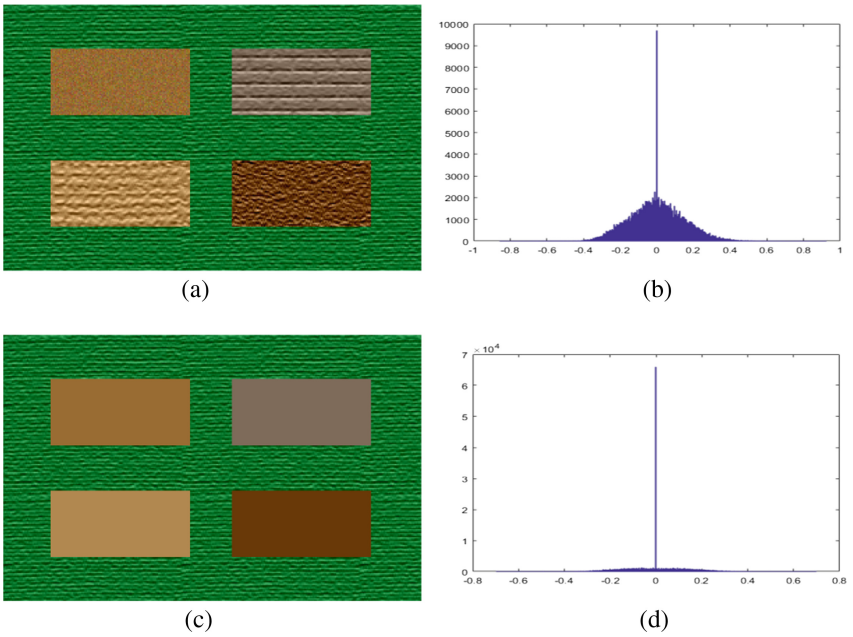

Fig. 3. Comparison of simulated farmland images and their histograms of gradient statistics before and after smoothing. (a) Original simulated image of farmland; (b) Histogram of gradient statistics of (a); (c) Ideal smoothed image of (a); (d) Histogram of gradient statistics of (c).

$$T(u) = \begin{cases} \nabla u = \sqrt{u_x^2 + u_y^2} & \nabla u < \varepsilon \\ \varepsilon & \text{otherwise} \end{cases} \tag{4}$$

$$s.t. \quad u(x, y) \in [0, 1]; x, y \in \Omega \tag{5}$$

Where $1/c$ is the normalization factor, ∇u is the gradient of u, Ω represents the region of the image. The formulas above indicate that only the gradient smaller than the threshold ε is calculated. The problem of obtaining the best smoothing result can be regarded as the Maximum a Posteriori estimation. When suppose the noise of image obeys zero mean Gaussian distribution ($(f - u) \sim N(0, \sigma^2)$), it can be expressed as

$$\begin{aligned} \arg\max L(u) &= \ln\left(\prod_{i=1}^{n} \frac{1}{\sigma\sqrt{2\pi}} e^{-\frac{(f_i - u_i)^2}{2\sigma^2}} \cdot \prod_{j=1}^{m} \frac{1}{c} e^{-|T(\nabla u)|}\right) \\ &= -\frac{1}{2\sigma^2} \sum_{i=1}^{n} (f_i - u_i)^2 - \sum_{j=1}^{m} |T(\nabla u)| - n \ln(\sigma\sqrt{2\pi}) - m \ln c \end{aligned} \tag{6}$$

$$\begin{aligned}\arg\min l(u) &= \lambda \sum_{i=1}^{n} (f_i - u_i)^2 + \sum_{j=1}^{m} |T(\nabla u)| \\ &= \lambda \|f - u\|_2^2 + \|T(\nabla u)\|_1\end{aligned} \tag{7}$$

The u that minimizes (7) is the smoothing result we want, which can be acquired by using the gradient descent algorithm to solve the corresponding Euler-Lagrange (E-L) equation. The E-L equation and its solving method are

$$2\lambda(u - f) - div(\frac{T(\nabla u)}{|T(\nabla u)|}) = 0 \tag{8}$$

$$\begin{cases} \dfrac{\partial u}{\partial t} = div(\dfrac{T(\nabla u)}{|T(\nabla u)|}) - 2\lambda(u - f) \\ u|_{t=0} = f \\ \lambda = \dfrac{1}{\sigma^2 |\Omega|} \displaystyle\int_{\Omega} div(\frac{T(\nabla u)}{|T(\nabla u)|}(u - f)dxdy \end{cases} \tag{9}$$

As shown in Fig. 2(d), the proposed image smoothing algorithm makes a good balance between the detail smoothing and the strong edge preserving.

Image Enhancement. In our proposed method, image enhancement includes two parts: region edge enhancement and overall image contrast enhancement.

In many natural scenes, the gray value of the region boundary varies a lot and may be close to the value inside each region. If we set the edges to the same grayscale value, some interference would be removed. Therefore, we apply edge detection and make the result fuses with smoothed image to achieve edge enhancement:

$$I = \alpha u + \beta e + \gamma \, (\alpha = 1, \, \beta \geq 1) \tag{10}$$

Where I, u and e represent the result of edge enhancement, smoothing and edge detection respectively, α, β, γ are weight factors. If the boundaries' gray values of e are significantly different, β should be set greater than one.

In Fig. 4, we compare edge enhancement results using Laplace, Canny, Prewitt and Sobel operator. As we can see in (a), Laplace operator is very sensitive to edges, the edge of noise and texture are detected at the same time. When using Canny operator, there is no difference in strength of the edge it detects, as shown in (b). Since we hope as few edges as possible to be detected within the field area, Sobel operator is a better choice, it can overcome the defect of above two methods, as shown in (d). The result of using Prewitt operator is similar to Sobel, but it's not as accurate as that of Sobel. The effect of edge enhancement is achieved by merging smoothed image and multiple times of edge detection result using Sobel operator, which can be seen in Fig. 5(a).

Histogram equalization can be adopted to enhance the whole image contrast by expanding the distribution of pixel intensity, the result using this method is shown in

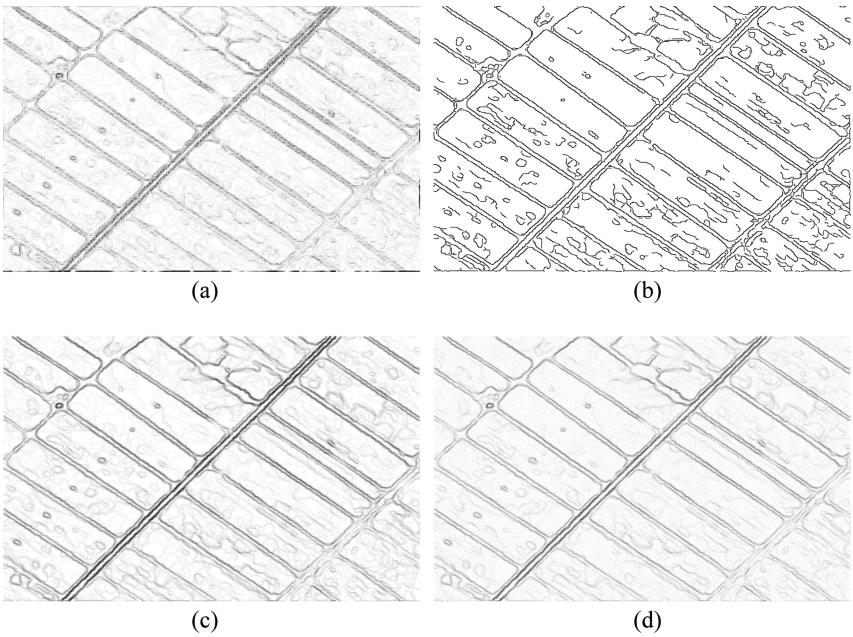

Fig. 4. Results comparison of edge detection for Fig. 1(a). (a) Laplace operator; (b) Canny operator; (c) Prewitt operator; (d) Sobel operator.

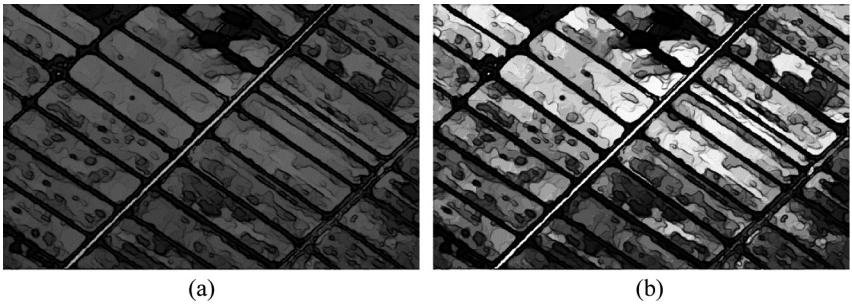

Fig. 5. Edge and whole image enhancement results. (a) Edge enhancement result with Sobel operator; (b) Image enhancement result with Histogram equalization.

Fig. 5(b). After image enhancement, the gray value of edges and other regions are clearly distinguished.

2.2 Image Segmentation

After the completion of image preprocessing, it is necessary to carry out the image segmentation before information extraction. We divide the process into two stages: threshold segmentation and region segmentation.

Threshold Segmentation. We want to make the edge and interior of regions in Fig. 5 (b) have the same gray value respectively, binarization in threshold segmentation is carried out first. However, the adaptive threshold algorithm which considered to have fine effect isn't perform better than fixed threshold segmentation when dealing with farmland images. The result after threshold segmentation is shown in Fig. 6(a).

Region Segmentation. After the fixed threshold segmentation, the edges of each region have been clearly depicted. However, there are some small black areas in the interior and white holes in the boundary line of individual regions, which are affected by the edge enhancement operation. If these interferences are removed, the farmland information extraction can achieve better. We adopted the region segmentation based on the region growth method to obtain the effect shown in Fig. 6(b). In order to retain valuable information, eight-neighborhood detection is selected to remove white holes, and four-neighborhood detection is selected to remove small black areas. If eight-neighborhood detection is still selected to remove the small black areas, the parts near the edge will not be easy to remove.

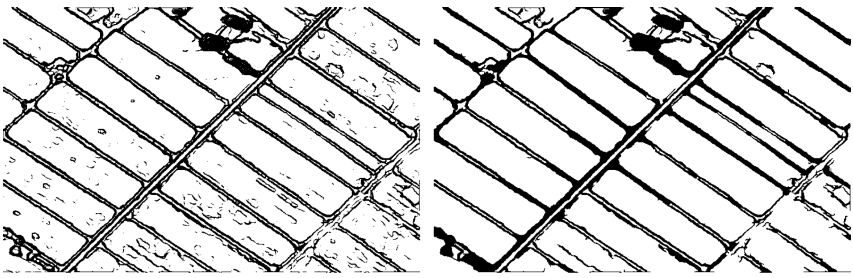

(a) (b)

Fig. 6. Image segmentation results. (a) Fixed threshold segmentation result. (b) Region segmentation result.

2.3 Information Extraction

In order to extract the information of the region of interest from the segmented image, the region needs to be separated from the whole image. Since the images we got at first are rasterized, we need to consider the process of converting raster regions into vector to reduce the amount of data and store results easily. Therefore, the information extraction process can be divided into region separation and vectorization.

Region Separation. According to the actual characteristics of the research object, we chose Flood fill method to realize the region separation, as shown in Fig. 7(a). Specifically, the eight-neighborhood detection method is used to obtain the mask image of the connected region with the same gray value, thus accelerating the processing.

Region Vectorization. Before this step, the separated images should be optimized by removing small black areas that away from edges. The Closing operation in the Mathematical morphology can be used and the kernel size can be selected as (5, 5).

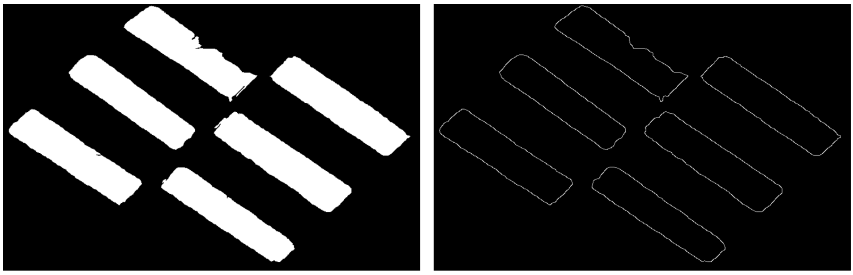

(a) (b)

Fig. 7. Results of region separation and contours. (a) Region separation result; (b) Thinning contours of regions tracked by the Freeman Chain Code.

Considering the complexity and efficiency of the algorithm, we choose the Freeman chain code to track the contour of regions (shown in Fig. 7(b)) to achieve vectorization.

The Freeman chain code picks any pixel point as a reference point, and gives different direction values to different neighbors of the pixel. When the value increases one, the direction it indicates rotates counterclockwise by 45°. The connected thinning contour is represented by chain code as follows:

$$F = (s, x, y, d_0, d_1, \ldots, d_j, \ldots, d_n, p) \tag{11}$$

Where F represents the string of chain code, s and p represent the start and end of the connected thinning contour respectively, (x, y) is the starting coordinate of the connected thinning contour, d_j is the direction code connecting the j *th* and the $j + 1$ *th* pixel of the connected thinning contour. The Freeman chain code only records the starting coordinate and direction code numbers, so it has simple data structure and stores a small amount of data.

Contour tracking is performed with the Freeman chain code for each connected thinning contour, and the gray value of the encoded pixels is set to zero to avoid repetition. After all pixels of thinning contours are removed, we can decode the chain codes and connect the pixels with line segments to obtain the vectorized images. When pixels connected by line segments are separated by 30 and 5 pixels, the effect is shown in Fig. 8(a) and (b). The final result of the proposed method of farmland segmentation and extraction with vectorization from raster images can be seen in Fig. 9(a). Each pixel we tracked can be recorded in the file for drawing the region boundaries directly later.

3 Study Area and Experimental Data

The RS images published on National Catalogue Service For Geographic Information website of China in 2012 were used to evaluate the effectiveness of the proposed method. The study areas are located in the countryside of Xianning (29.87 °N, 114.28 °E), Hubei province and Jiuquan (39.71 °N, 98.5 °E), Gansu province, China.

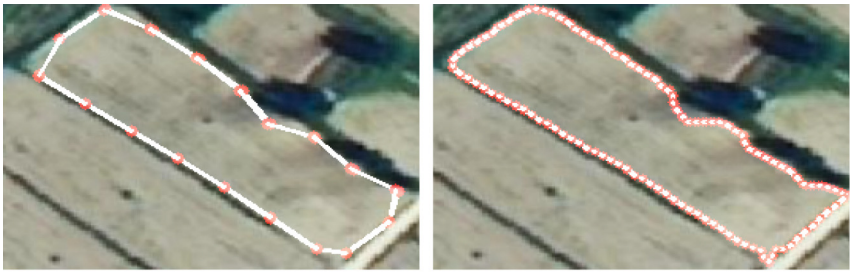

(a) (b)

Fig. 8. Information extraction results at different sampling intervals. (a) Line segments separated by 30 pixels; (b) Line segments separated by 5 pixels.

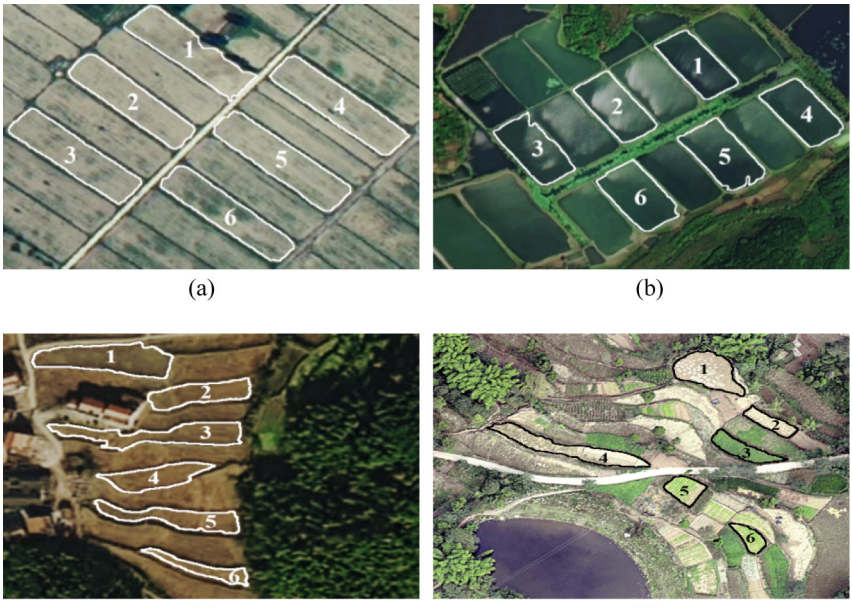

(a) (b)

(c) (d)

Fig. 9. Original aerial RS test images and the final results using the proposed method of regions selected randomly on the original images. (a), (b), (c), and (d) are typical rural landscape with different features of farmland captured by UCXP and are numbered on each region.

The typical images we chose to use are all parts of aerial RS images captured by UCXP, which has 0.1-m spatial resolution. As shown in Fig. 9, (a) is a part of farmland with colorful rectangular blocks in Jiuquan, (b) shows regular ponds with cloud reflections in Xianning, (c) is chosen to represent the irregular farmland, and (d) represents typical rural landscape with irregular farmland that has textural features, bending roads and randomly distributed trees.

Each image in Fig. 9 represents a typical farmland situation, as we can see, it is increasingly difficult to segment and extract the information of farmland areas we interested in. The more irregular the region is, the more textures there are in the region, and the more external disturbances such as vegetation and buildings are, the more complex the processing process will be.

4 Experimental Results

In order to analyze the effect of the proposed method, we designed an experiment to test the accuracy of information extraction. The experimental hypothesis is that the boundary of farmland region depicted manually is completely accurate and the extracted region information is complete. Experimental steps:

- Paint boundaries of areas which are easy for the human to distinguish in the raster RS image manually and obtain the boundaries of the same regions with the proposed method in this paper, then fill the interior of boundaries obtained in different ways.
- Number the regions (as shown in Fig. 9) and input the filling images of these two methods into the region separation process of the proposed method to obtain the number of pixels filled in each region. The way of calculating the accuracy is:

$$A = [1 - |(N - N_0)/N_0|] \times 100\% \tag{12}$$

Where A represents the accuracy, N_0 represents the number of pixels filled in each hand-painted region, and N represents the number of pixels in the region filled with the proposed method.

The segmentation and extraction results using the proposed method of the sample images are shown in Fig. 9. According to the number of areas shown in each image, the above experimental method was applied, and statistical results are shown in Table 1.

Table 1. The experimental results of the method we presented.

		1	2	3	4	5	6	AVG
Fig. 9(a)	N_0	15674	15653	17235	17821	18252	15974	98.67%
	N	16294	15874	17069	17950	18357	16029	
	A	96.04%	98.59%	99.04%	99.28%	99.42%	99.66%	
Fig. 9(b)	N_0	10774	11296	11214	11389	12400	11818	97.48%
	N	11080	11601	11326	11703	12585	12333	
	A	97.16%	97.30%	99.00%	97.24%	98.51%	95.64%	
Fig. 9(c)	N_0	6582	3785	5520	3429	4791	2421	91.12%
	N	7077	4118	6277	4046	4560	2410	
	A	92.48%	91.20%	86.29%	82.01%	95.18%	99.55%	
Fig. 9(d)	N_0	6026	2398	3165	7189	3795	1856	89.53%
	N	6496	2554	3517	7353	2822	2032	
	A	92.20%	93.49%	88.88%	97.72%	74.36%	90.52%	

The average accuracy of the method proposed in this paper is 94.2%, but as we can see, the accuracy decreases with the increase of texture and shadow interference. The fifth region in Fig. 9(d) has the lowest accuracy because the method doesn't have the ability to think like a person that two parts with very different gray values are actually a region.

5 Conclusion

In this paper, we have presented a new approach for farmland segmentation and extraction from raster RS images. The experimental results demonstrate that the whole process proposed in this paper can achieve considerable success even regions are colorful, irregular and have textures inside. When the contrast between the interior and the boundary of a region is distinct, the accuracy of the extraction can be relatively high. However, when the boundary of a region is affected by the shadow of vegetation or farmland, or the gray value of texture within the region varies greatly, the extracted results will have much deviation, which is another important research topic to be solved. In a word, the proposed method has a considerable effect on the segmentation and extraction of farmland regions, and can be extended to other areas, such as roads, buildings, water areas, etc.

References

1. Marr, D., Hildreth, E.: Theory of edge detection. Proc. R. Soc. Lond. Biol. Sci. **207**(1167), 187–217 (1980)
2. Tomasi, C., Manduchi, R.: Bilateral filtering for gray and color images. In: Sixth International Conference on Computer Vision, pp. 839–846. IEEE, India (1998)
3. Rudin, L.I., Osher, S., Fatemi, E.: Nonlinear total variation based noise removal algorithms. Physica D **60**(1–4), 259–268 (1992)
4. Farbman, Z., Fattal, R., Lischinski, D., Szeliski, R.: Edge-preserving decompositions for multi-scale tone and detail manipulation. ACM Trans. Graph. **27**(3), 67 (2008)
5. Zhang, Q., Shen, X., Xu, L., Jia, J.: Rolling guidance filter. In: Fleet, D., Pajdla, T., Schiele, B., Tuytelaars, T. (eds.) ECCV 2014. LNCS, vol. 8691, pp. 815–830. Springer, Cham (2014). https://doi.org/10.1007/978-3-319-10578-9_53
6. Dou, Z., Song, M., Gao, K., et al.: Image smoothing via truncated total variation. IEEE Access **5**, 27337–27344 (2017)
7. Chen, Q., Luo, J., Zhou, C., et al.: A hybrid multi-scale segmentation approach for remotely sensed imagery. In: 2003 IEEE International Geoscience and Remote Sensing Symposium, pp. 3416–3419. IEEE, France (2003)
8. Yang, J., He, Y., John, C.: A self-adapted threshold-based region merging method for remote sensing image segmentation. In: 2016 IEEE International Geoscience and Remote Sensing Symposium, pp. 6320–6323. IEEE, Beijing (2016)
9. Song, Y., Wu, Y., Dai, Y.: A new active contour remote sensing river image segmentation algorithm inspired from the cross entropy. Digit. Sig. Process. **48**, 322–332 (2016)

10. Jin, H., Feng, Y., Li, B.: Road network extraction with new vectorization and pruning from high-resolution RS images. In: 2008 23rd International Conference Image and Vision Computing New Zealand, pp. 1–6. IEEE, New Zealand (2008)
11. Xu, L., Ming, D., Zhou, W., et al.: Farmland extraction from high spatial resolution remote sensing images based on stratified scale pre-estimation. Remote Sens. **11**(2), 108 (2019)